Vietnam Journal of Science and Technology ***61*** *(3) (2023) 394-404*

doi:10.15625/2525-2518/16892

Synthesis of highly stable silver nanoparticles as computed tomography contrast agents

Nguyen Thi Ngoc Linh[1], Le The Tam[2, *]

[1]*Thai Nguyen University of Sciences, Tan Thinh Ward, Thai Nguyen City, Thai Nguyen Province, Viet Nam*

[2]*Vinh University, 182 Le Duan, Vinh City, Nghe An Province, Viet Nam*

[*]Emails: *tamlt@vinhuni.edu.vn*

Received: 23 January 2022; Accepted for publication: 8 April 2022

Abstract. In this work, a highly stable solution of Ag nanoparticles was synthesized by reduction method using poly(acrylic acid) (PAA) as a phase transition ligand in organic solvents. The effects of different solvents on the morphology and properties of the Ag nanomaterials were investigated in detail. The structural analysis demonstrated that the Ag nanomaterials showed good crystallinity. We have successfully synthesized Ag nanoparticles (Ag NPs) with small particle size (6.1 - 7.3 nm) and high uniformity in organic solvents at room temperature. The Ag NPs obtained after phase transformation with PAA had good dispersibility, endurance and stability in aqueous solvents. The obtained *in-vitro* CT imaging results showed a good X-ray absorption value. These findings suggested the potential application of PAA-coated Ag nanoparticles in the biomedical field, especially in imaging diagnostics using computed tomography.

Keywords: nanomaterials, Ag NPs, computed tomography (CT), reduction in organic solvents, poly (acrylic acid) (PAA)

Classification numbers: 2.2.1, 2.4.3.

1. INTRODUCTION

Computed tomography (CT) is an X-ray-based imaging technique that is applied to scan a body part that requires a cross-sectional examination, and then coordinates with a computer to produce 2 or 3 dimensional images of the part to be taken. This is considered an effective method to help doctors examine and diagnose diseases accurately. The currently clinically approved contrast agents for CT are iodized small molecules [1, 2]. They are effective in absorbing X-rays, but have the disadvantage of a nonspecific distribution and pharmacokinetics that are rapidly removed from the blood. Besides, there is also a limitation in targeting tissues within organs, which is not a specific agent for any disease or diseased tissue [3]. Especially, iodine-containing contrast agents are often associated with allergic reactions and are contraindicated in patients with kidney disease [4 - 7]. Due to the limitations of iodinated contrast agents, recently, along with the development of nanotechnology, studies on the

application of nanoparticles as an alternative contrast agent in CT scanning have been strongly reported as an attempt to develop new contrast agents with more advantages. In which, the heavy metal elements have a high atomic number as well as a regular absorption coefficient in equivalent with or even higher than that of a standard iodinated contrast agent and thus provide greater contrast per weight. Their nanoparticles with the ability to absorb X-rays have been attracting much attention in the field of CT imaging [8 - 10]. Therefore, currently nanoparticles of precious metals or their compounds are also included in CT imaging for tumor detection and drug delivery [11, 12]. However, these nanomaterials are generally not used independently for drug delivery, diagnosis and treatment because of their poor biocompatibility surface, high toxicity and poor absorption of small molecules [13, 14]. Therefore, it is necessary to explore polymer-coated nanomaterials or nanoparticles with low toxicity, high biocompatibility and specific surface area for improvement [14, 15].

The development of gold nanoparticles (Au NPs) as a CT contrast agent is currently a topic of intense interest among precious metal nanocontrasts. Au NPs have many favorable properties for this application such as the large capacity of contrast-created material, strong X-ray attenuation, adjustable material size and shape, high biocompatibility, and mutable chemical surface [9, 16]. However, one disadvantage of Au NPs-based contrast agents is their high cost. Meanwhile, Ag NPs have many useful biological features, such as antibacterial, antiviral and antifungal [17 - 19]. In addition, the unique optical properties of AgNPs have also been applied to the development of sensors, imaging agents and treatment methods [20, 21]. Recently, the X-ray blocking property of Ag NPs has been used for CT imaging as a novel method in the search for novel diagnostic agents [21, 22]. The gray levels in the CT section images correspond to X-ray attenuation, reflecting the proportion of X-rays scattered or absorbed as they pass through each voxel and are influenced by the density and composition of the material being taken a photo. The silver atoms can produce strong X-ray attenuation due to their high electron density (10.49 g/cm^3) and high X-ray absorption coefficients (X-ray absorption coefficient at 100 keV, Ag 1.47 cm^2/g), which makes the Ag nanoparticles may in the future become an ideal contrast agent for computed tomography (CT) instead of conventional iodine-based contrast agents. Currently, there have been a number of studies on the use of Ag NPs as CT contrast agents [22 - 24]. However, the Ag NPs used in these studies have a large mean size and a fairly wide size distribution with a mean size of 21 ± 8 nm. Although, Ag NPs have a lot of promise in CT imaging, studies on the X-ray absorption capacity of Ag NPs are still very limited, on the other hand, the improvement of surface modification of Ag NPs has many aspects yet to be clarified. In addition, the synthesis of size-controled and uniform Ag nanoparticles is difficult to achieve. In this study, we investigated the influence of some organic solvents on the particle size and dispersion of Ag nanoparticles at room temperature. The Ag nanoparticles in the organic solvent are then subjected to a phase-transferred process with poly(acrylic acid) (PAA) ligand followed by surface functionalization with COOH group in order to form a stable and homogeneously dispersed colloidal system in water. Simultaneously, the Ag NPs surface was modified with poly (acrylic acid) (PAA) with good biocompatibility, thereby initially evaluating its ability as a contrast agent in in-vitro CT imaging.

2. MATERIALS AND METHODS

2.1. Materials

All chemicals used in the fabrication process were of analytical grade (purchased from Sigma-Aldrich Ltd, Singapore) with purity ≥ 99 %, including: silver nitrate ($AgNO_3$),

oleylamine (OLA), *tert*-butylamine borane (TBAB); 1,2,3,4-tetrahydronaphthalene (tetralin), 1-octadecene (ODE), 1,2-dichlorobenzene (DCB), poly (acrylic acid) (PAA), ethanol and *n*-hexane.

2.2. Synthesis of Ag NPs by reduction method in organic solvents

In this study, highly stable Ag nano liquid was synthesized for biomedical application including two stages as depicted in scheme 1 [25]. In the first step, Ag nanoparticles were fabricated using TBAB to reduce Ag^+ in the presence of OLA in organic solvents at room temperature. The Ag nanoparticles synthesized were covered with a layer of hydrophobic OLA surfactant. In biomedical applications, they must be dispersed stably in aqueous solvents. Therefore, Ag NPs were well dispersed into water using poly(acrylic acid) as the phase transfer ligand in step 2.

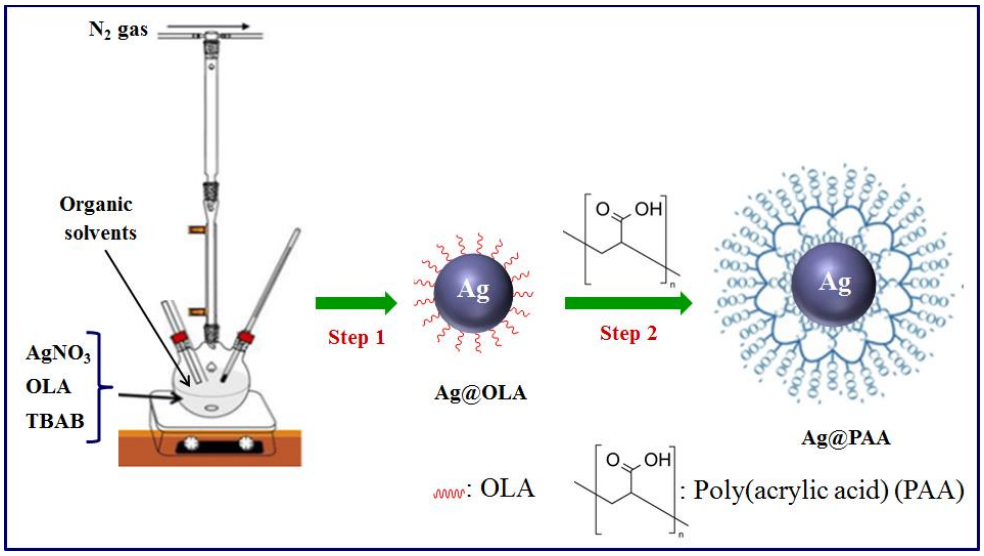

Scheme 1. Schematic synthesis of Ag nanoparticles by reduction method in organic solvents and the ligand exchange process using PAA.

Ag nanoparticles were synthesized in organic solvents at room temperature according to the following procedure: Place 0.75 g of $AgNO_3$ and 6 mL of OLA into a 3-necked flask containing 30 mL of organic solvent (tetralin, ODE or DCB). The reaction mixture was stirred under a stream of N_2 gas until completely dissolved. A reducing agent solution containing 0.0435 g of TBAB, 1 mL of OLA, and 1 mL of organic solvent (tetralin, ODE or DCB) was stirred by ultrasonic vibration at room temperature, then slowly added to the solution in the flask and the reaction was carried out for 60 min at room temperature.

Ag nanoparticles were filtered and thoroughly washed with ethanol. Then, the washed Ag nanoparticles were dispersed in 1 mL of n-hexane solvent.

2.3. Phase transition of Ag NPs by ligand exchange using PAA

The phase transfer process of Ag nanoparticles from hydrophobic phase to hydrophilic phase was performed according to the method in our previous works [26]: Disperse 2 g of PAA in 40 mL of triethylene glycol (TEG) at 110 °C to obtain solution A. 100 mg of Ag nanoparticles

were dispersed in 5 mL of n-hexane, forming solution B, which was then quickly added to solution A. The resulting mixture was heated up to 280 ^{o}C at a rate of 3 °C/minute and kept at this temperature for 6 hours. The mixture was then cooled to room temperature. The Ag nanoparticles after PAA coating (Ag@PAA) were separated from the solution by adding dilute ethyl acetate and centrifuged at 12000 rpm. Finally, the Ag@PAA nanoparticles were re-dispersed in water by ultrasonic waves to obtain a solution of Ag nanoparticles.

2.4. Characterization methods of Ag NPs

The morphology and size of Ag nanoparticles were determined by transmission electron microscopy (TEM) on the JEM 1010 device (Japan). The crystalline phase analysis was carried out on an X-ray diffractometer – SIEMENS D5005 using radiant Cu K_{α} (λ = 1,5406 Å). The UV-Vis spectra of the samples were recorded on a Jasco V-670 spectrometer (Japan). The hydrodynamic size (DLS) and Zeta potential of the Ag nanoparticles in the study were determined by dynamic light scattering method on the Zetasizer - Nano ZS device of Malvern - UK.

2.5. In-vitro CT samples preparation

To determine the potential of Ag NPs for use in CT imaging, imaging wells were prepared with agarose gel for sample fixation, by dissolving 1 g of agarose in 100 mL of distilled water at 80 °C. Then, 1 mg of Ag NPs was dispersed in 700 µL of distilled water and then 300 µL of hot agarose solution was added to the mixture in a 2 mL well. Five gel wells containing different amounts of Ag NPs (0.5, 1, 2, 3 and 5 mg/mL) were prepared together with a blank agarose gel well (control). The samples were kept at room temperature until solidified. A 128-Somatom Perspective CT scanner (Siemens, Germany) was used to scan CT samples with the following imaging parameters [22, 23, 27]: Source voltage 130 kV, 80 mAs, slice thickness 0.5 mm, the field of view DFOV x-y 270 × 270 mm^2, matrix size 480 × 480. To determine the HU value, measurements were performed (region of interest - ROIs) (cm^2) on eFilm workstations (Merge Healthcare, Chicago, IL, USA).

3. RESULTS AND DISCUSSION

3.1. Influence of solvents on the morphology and optical properties of the Ag NPs

The morphology of Ag NPs can be controlled by the nucleation and growth process [28]. This process is strongly influenced by synthetic factors such as precursor concentration, solvent, etc. [29]. In this study, we investigated the influence of some organic solvents on the morphology and size of Ag nanomaterials. The results of the analysis by transmission electron microscopy (TEM) are shown in Figure 1. It was found that the Ag nanoparticles synthesized in tetralin solvent werespherical in shape, relatively uniform, and had clear grain boundaries, an average particle size of 6.4 ± 0.8 nm, and a standard deviation (stdev) of 12.5 % (Figure 1a). The Ag NPs fabricated in ODE solvent were spherical particles, very uniform, with clear grain boundaries and an average particle size of 6.1 ± 0.5 nm, and the stdev in this case (8.2 %) was quite small (Figure 1b). With DCB solvent, the obtained Ag nanoparticles had unclear grain boundaries, an average particle size of 7.3 ± 1.2 nm, and a high stdev of 16.4 %. (Figure 1c). Thus, all three solvents used in the synthesis process gave Ag NPs in spherical shape, with a particle size below 10 nm and uniformity depending on the solvent used (Figure 1d). The ODE

solvent was favorable for the formation of Ag nanoparticles with high uniformity and the smallest particle size, while tetralin and DCB solvents gave less uniform particles with larger particle size. This result can be explained by the influence of tetralin and DCB solvent molecules with bulky structure, which affects the crystal nucleus formation and the growth of Ag nanomaterials.

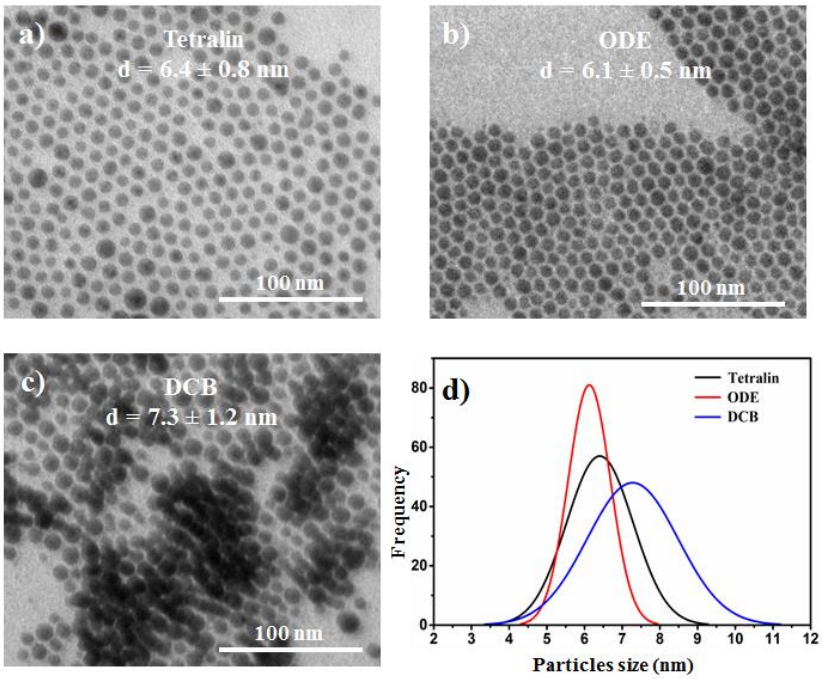

Figure 1. Typical TEM images (Scale bar: 100 nm) of Ag NPs in different solvents (a-c) and corresponding size distribution histograms (d).

The optical properties of Ag nanoparticles prepared in different solvents were studied by UV-Vis spectroscopy (Figure 2a). The results indicated that the samples showed a surface plasmon resonant range with high absorption intensity characteristic for the Ag element. The surface plasmon resonance (SPR) positions of the fabricated Ag nanoparticles ranged from 399 to 400 nm. According to Mie theory [30], there is only a single SPR site in the absorption spectrum of spherical metal nanoparticles, while anisotropic particles can produce two or more SPR peaks depending on the shape of particles. In this case, only a single SPR position was observed, demonstrating that the obtained Ag nanoparticles were spherical in shape. This finding was convinced by the results of the transmission electron microscopy (TEM) method as shown in Figure 1.

The crystallinity of Ag NPs was examined by X-ray diffraction pattern as shown in Figure 2b. The analytical results showed that all samples contained only Ag NPs with high crystallinity with face-centered cubic structure (fcc) including characteristic pictures at positions $2\theta = 38.20^{o}$; 44.2^{o} and 64.21^{o} that correspond to crystal planes (111), (200) and (220) characteristic for Ag crystals (JCPDS, 004-0783). Figure 2b shows an X-ray diffraction pattern of a representative sample of Ag nanocomposites synthesized in ODE solvent. The average crystal size of 6.0 nm was obtained from the (111) peak expansion. This result meets the TEM image analysis results presented in Figure 1b as 6.1 ± 0.5 nm.

Among the investigated solvents, ODE was a favorable solvent for the formation of nanoparticles with a small particle size (6.1 nm), high uniformity, and a small particle size error (8.2 %), so this was used to transfer phase and study the stability of the Ag nanoparticles solution.

FT-IR spectroscopy was characterized to confirm the interaction between PAA and Ag nanoparticles (Figure 2c).

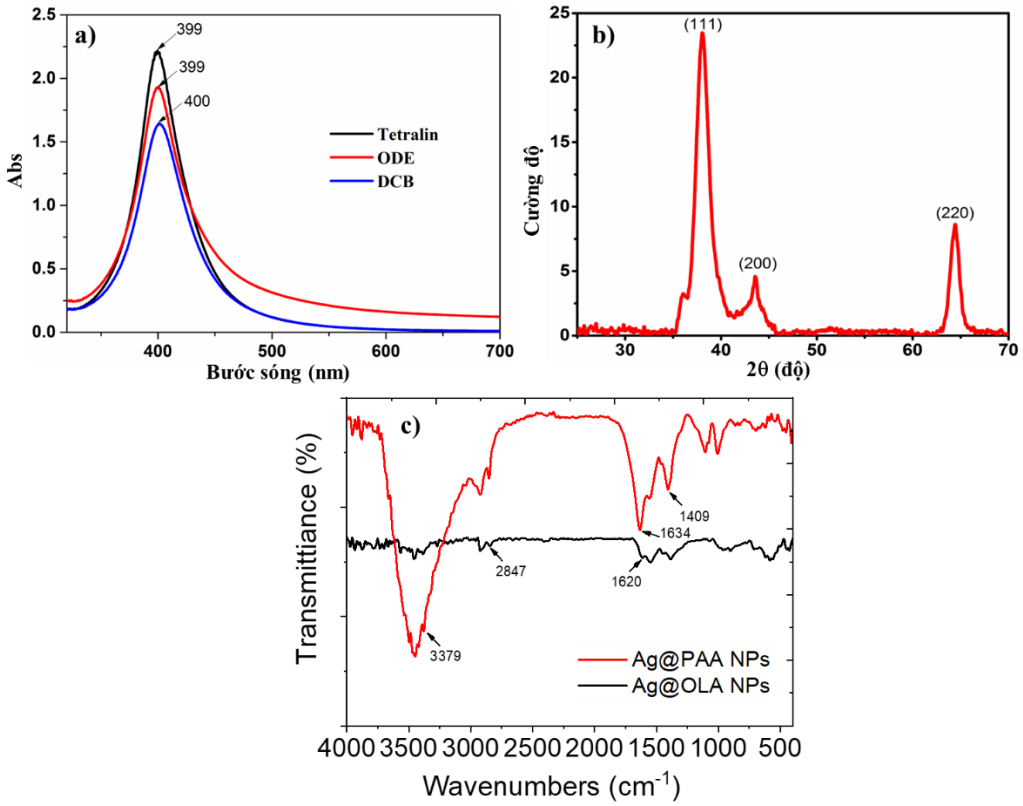

Figure 2. UV-vis absorption spectra of Ag NPs (a); XRD patterns of Ag NPs synthesized in ODE solvents (b) and FTIR spectra of Ag NPs, Ag@PAA NPs (c).

It can be seen that the absorption peak at 2847 cm^{-1} represents the vibration of C-H groups in the OLA molecule. A weak stretching band at 1620 cm^{-1} is assigned to the deforming fluctuation of NH_2 complex of the OLA molecule. These results confirm that OLA uniformly covers the surface of Ag nanoparticles. The IR spectrum of Ag@PAA shows two strong peaks at 3379 cm^{-1} và 1634 cm^{-1}, which are assigned to the typical stretching vibrations of O-H and C=O of -COOH group in the IR spectrum of Ag@PAA, respectively. Moreover, the occurrence of vibration peaks characteristic of the carboxyl group (1409 cm^{-1}) on the FT-IR spectrum again confirmed the presence of the PAA coating.

3.2. Particle size and stability of the PAA-coated Ag NPs

To be used as biomedical materials, Ag nanoparticles must be well dispersed and stable in an aqueous solvent. The colloidal stability of Ag nanoparticles depends on a number of

parameters such as particle size and functional groups on the surface of the nanoparticles. In this study, we use PAA polymer as a phase transfer ligand for Ag nanoparticles from hydrophobic to hydrophilic. The results showed that, before phase transition, Ag nanoparticles were well dispersed in n-hexane and not in water. After phase transition with PAA, the surface of Ag nanoparticles became hydrophilic, so they dispersed well in an aqueous solvent (Figure 3a). The TEM images (Figure 3b) indicate that Ag@PAA nanoparticles are spherical in shape, monodispersed, and non-agglomerated.

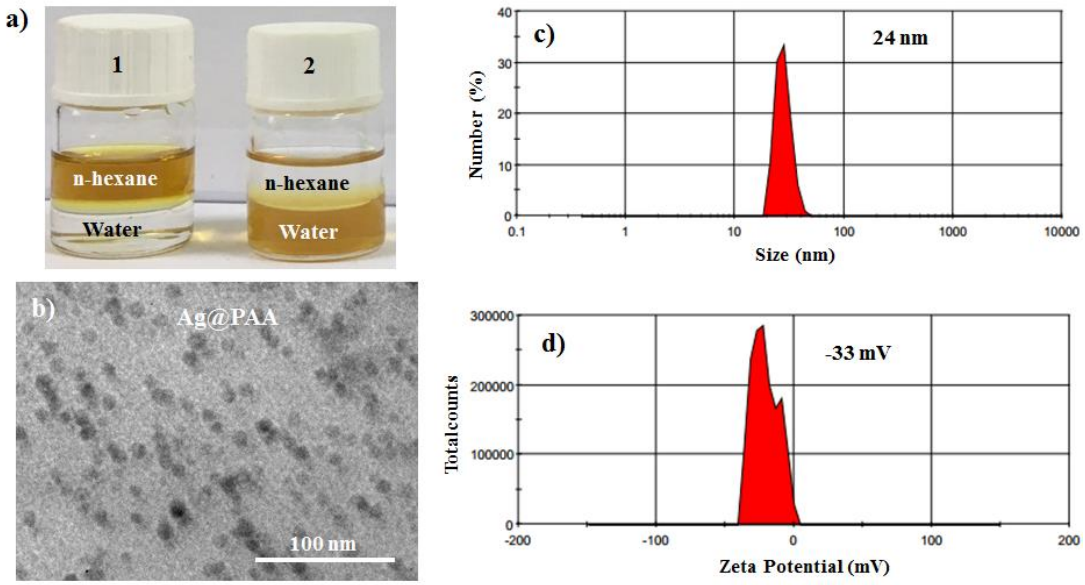

Figure 3. The images of Ag NPs before and after phase tranfer by PAA (a); the TEM image of PAA encapsulated Ag NPs (b); hydrodynamic size distribution (c) and Zeta potential of the PAA-coated Ag NPs (d).

To evaluate the stability of Ag@PAA nanoparticles in aqueous solvents, we measured the hydrodynamic size of the NPs by the dynamic light scattering method (DLS). The results in Figure 3c show a peak at 24 nm with a narrow bottom width indicating that the Ag nanoparticles coated with PAA are relatively uniform with an average size of 24 nm. Besides, the solution of Ag@PAA nanoparticles is highly stable with a Zeta potential value of -33 mV (Figure 3d). The research results show that the Ag nano liquid synthesized in this study is suitable for biomedical applications.

3.3. In-vitro CT imaging

The use of Ag NPs as CT contrast agents is notable because they cause comparable X-ray in equivalent with iodine-based CT in terms of atomic number. To explore the CT imaging potential, the X-ray attenuation properties of Ag NPs nanoparticles were also investigated to confirm their use as contrast agents in CT imaging. Similar to the MRI image signal acquisition technique, in CT imaging technique the HU values of the acquired images will be directly analyzed using eFilm workstations software (Merge Healthcare, Chicago, IL, USA) based on the signal strength of the received region of interest (ROIs). Figure 4 shows the CT image using Ag NPs nanoparticles at different Ag concentrations (a) and the linear plot of the Hounsfield unit relative to the Ag concentration (b). The results showed that, with increasing Ag concentration,

the CT image intensity increased linearly, corresponding to the increased value of Hounsfield intensity.

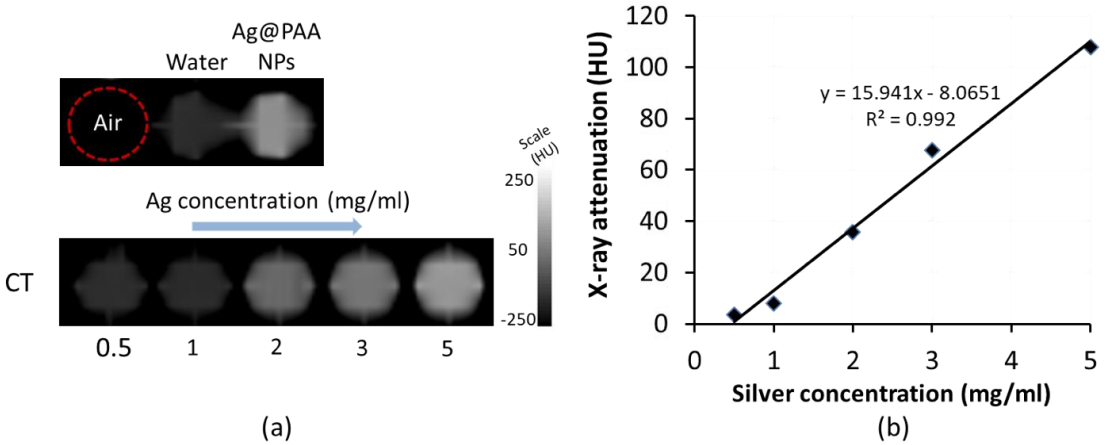

Figure 4. Computed tomography (CT) image of the Ag@PAA NPs with different concentrations (0.5, 1, 2, 3 and 5 mg/mL) and X-ray attenuation intensity (HU).

When compared with MRI imaging techniques, CT exhibits low sensitivity in the absence of contrast stain (contrast agent) and is therefore limited. The X-ray attenuation of Ag NPs increased linearly with Ag concentration and volume. Figure 4a describes a clearly visible contrast for the nanoparticle samples with Ag concentrations starting from 2 mg/mL. When the Ag concentration increased from 1 mg/mL to 2 mg/mL, the X-ray absorption capacity increased linearly, corresponding to a strong increase in signal intensity from 7.9 HU to 35.9 HU (4.5 times increase). The table-based quantification of mean gray scale values showed a linear correlation between the obtained CT contrast and the nanoparticle concentration as expected (R^2 = 0.992) (Figure 4b). The X-ray attenuation characteristic of Ag nano was compared with those for water and air to clearly see the X-ray absorption ability of the material. The results in Figure 4a show that the X-ray absorption capacity was strong, specifically, the hounsfield signal intensity for air ranged from -900 HU to -1000 HU, in the presence of water the signal increased to 0 HU, while for the case of Ag nanoparticles it increased to 107.8 HU. Comparing the hounsfield units (HU) of Ag NPs with Au NPs and iodine-based contrast agents in CT imaging shows that the Ag NPs contrast agent did not give much different signal. For example, in the study of Yuxi C. Dong *et al*., the Au NPs concentration varied from 0.5 to 10 mg/mL, corresponding to the Hounsfield signal intensity increasing from 30 HU to 270 HU, respectively [9]. The study by Mohammed Ali Dheyab *et al*. showed that to achieve the Hounsfield signal intensity of 178 HU, the concentration of Au NPs and Iodine (in the commercial drug Omnipaque) must reach 2.3 mg/mL and 7.2 mg/mL, respectively [8]. Therefore, the in vitro (HU) tests showed that the PAA surface-denatured Ag NPs nanoparticles can be used as an alternative contrast agent for CT imaging.

4. CONCLUSIONS

We have successfully synthesized Ag nanoparticles with a small particle size (6.1 - 7.3 nm) and high uniformity in organic solvents at room temperature. The reaction solvent had an

influence on the size, uniformity and optical properties of the Ag nanoparticles. The Ag nanosolution obtained after phase transformation with PAA had good dispersion, endurance and stability in aqueous solvents. The obtained in-vitro CT imaging results demonstrated a good X-ray absorption value, showing that Ag NPs had the potential to be used as a CT contrast agent in which their X-ray attenuation was linearly correlated with the Ag NPs concentration. This research result opens up the potential application of Ag nanoparticles in the biomedical field, especially in imaging diagnostics using computed tomography.

Acknowledgment. Le The Tam was funded by Vingroup JSC and supported by the Postdoctoral Scholarship Programme of Vingroup Innovation Foundation (VINIF), Institute of Big Data, code VINIF.2021.STS.10.

CRediT authorship contribution statement. Le The Tam, Nguyen Thi Ngoc Linh: Synthesis, analysis and assessment of morphology and structure of materials; Nguyen Thi Ngoc Linh: Writing - original draft; Le The Tam: Supervision, Writing - review and editing. All authors read and approved the final manuscript.

Declaration of competing interest. There are no conflicts to declare.

REFERENCES

1. Rutten A., Prokop M. - Contrast Agents in X-Ray Computed Tomography and Its Applications in Oncology, Anticancer, Agents Med. Chem. **7** (2007) 307. https://doi.org/10.2174/187152007780618162.
2. Beckett K. R., Moriarity A. K., Langer J. M. - Safe use of contrast media: What the radiologist needs to know, Radiographics **35** (2015) 1738. https://doi.org/10.1148/rg.2015150033
3. Hoffmann M. H. K. - Contrast Agent Application and Protocols, Multislice CT. **8** (2008) 97. https://doi.org/10.1007/174_2011_406.
4. Mehrizi M., Pascuzzi R. M. - Complications of radiologic contrast in patients with myasthenia gravis, Muscle and Nerve. **50** (2014) 443. https://doi.org/10.1002/mus.24254.
5. Barrett B. J., Parfrey P. S. - Preventing Nephropathy Induced by Contrast Medium, N. Engl. J. Med. **354** (2006) 379. https://doi.org/10.1056/NEJMcp050801.
6. Lasser E. C., Lyon S. G., Berry C. C. - Reports on contrast media reactions: Analysis of data from reports to the U.S. Food and Drug Administration, Radiology **203** (1997) 605. https://doi.org/10.1148/radiology.203.3.9169676.
7. Hitoshi K., Koichi Y., Takahiro K., Tsutomu T., Peter S., Keiichi. M. - Adverse reactions to ionic and nonionic contrast media, J. Emerg. Med. **175** (1990) 621. https://doi.org/10.1148/radiology.175.3.2343107.
8. Dheyab M. A., Aziz A. A., Jameel M. S., Khaniabadi P. M., Oglat A. A. - Rapid sonochemically-assisted synthesis of highly stable gold nanoparticles as computed tomography contrast agents, Appl. Sci. **10** (2020) 7020. https://doi.org/10.3390/app10207020.
9. Dong Y. C., Maryam H., Maidment P. S. N., Jessica C. H., Pratap C. N., Salim M., Marine B., Johoon K., Peter C., Philippe D., Harold I. L., David P. C. - Effect of Gold Nanoparticle Size on Their Properties as Contrast Agents for Computed Tomography, Sci. Rep. **9** (2019) 14912. https://doi.org/10.1038/s41598-019-50332-8.
10. Mahan M. M., Doiron A. L. - Gold Nanoparticles as X-Ray, CT and Multimodal Imaging

Contrast Agents: Formulation, Targeting, and Methodology, J. Nanomater. **2018** (2018) 5837276. https://doi.org/10.1155/2018/5837276.

11. Kong, F. Y., Zhang J. W., Li . F., Wang Z. X., Wang W. J. and Wang W. - Unique roles of gold nanoparticles in drug delivery, targeting and imaging applications, Molecules. **22** (2017) 1445. https://doi.org/10.3390/molecules22091445.
12. He H., Yang D. P., Liu. M., Wang X., Zhang Z., Zhou G., Liu W., Zhang C. Y., Wen J. - pH-sensitive Au - BSA - DOX - FA nanocomposites for combined CT imaging and targeted drug delivery, Int. J. Nanomedicine**. 12** (2017) 2829. https://doi.org/ 10.2147/IJN.S128270.
13. Arvizo R., Bhattacharya R., Mukherjee P. - Gold nanoparticles: Opportunities and challenges in nanomedicine, Expert Opin. Drug Deliv.**7** (2010) 753. https://doi.org/ 10.1517/17425241003777010.
14. Kim, D., Park, S., Jae, H. L., Yong, Y. J., Jon, S. - Antibiofouling polymer-coated gold nanoparticles as a contrast agent for in vivo X-ray computed tomography imaging, J. Am. Chem. Soc. **129** (2007) 7661. https://doi.org/10.1021/ja071471p.
15. Hu, X., Zhang, Y., Ding, T., Liu, J., Zhao H. - Multifunctional Gold Nanoparticles: A Novel Nanomaterial for Various Medical Applications and Biological Activities, Front. Bioeng. Biotechnol. **8** (2020) 990. https://doi.org/10.3389/fbioe.2020.00990.
16. N. T. Dung., Nguyen T. N. Linh., Dinh L. Chi., Nguyen T. H. Hoa., Nguyen P. Hung., Ngo T. Ha., Pham H. Nam., Nguyen X. Phuc., Le T. Tam and Le. T. Lu. - Optical properties and stability of small hollow gold nanoparticles, RSC Adv. **11** (2021) 13458. https://doi.org/10.1039/D0RA09417J.
17. Kim J. S., Kuk. E., Yu. K. N., Kim J.H., Park S. J., Lee H. J., Kim S. H., Park Y. K., Park Y. H., Hwang C. Y., Kim Y.K., Lee Y.S., Cho M.H. - Antimicrobial effects of silver nanoparticles, Nanomedicine Nanotechnology, Biol. Med. **3** (2007) 95. https://doi.org/ 10.1016/j.nano.2006.12.001.
18. Galdiero, S., Falanga A., Vitiello M,. Cantisani M., Marra V., Galdiero M. - Silver nanoparticles as potential antiviral agents, Molecules. **16** (2011) 8894. https://doi.org/10.3390/molecules16108894.
19. Lee S. H., Jun B. H. - Silver nanoparticles: Synthesis and application for nanomedicine, Int. J. Mol. Sci. **20** (2019) 865. https://doi.org/10.3390/ijms20040865.
20. Sabela M., Balme S., Bechelany M., Janot J. M., Bisetty K. - A Review of Gold and Silver Nanoparticle-Based Colorimetric Sensing Assays, Adv. Eng. Mater. **19** (2017) 1700270. https://doi.org/10.1002/adem.201700270.
21. Ramesh, S., Grijalva M., Debut A., Torre B. G., Albericio F., and Cumbal L. H. - Peptides conjugated to silver nanoparticles in biomedicine-a 'value-added' phenomenon, Biomater. Sci. **4** (2016) 1713. https://doi.org/10.1039/C6BM00688D.
22. Zou, J., Hannula M., Misra., Feng H., Labrador R. H., Aula A. S., Hyttinen J., and Pyykkö I. - Micro CT visualization of silver nanoparticles in the middle and inner ear of rat and transportation pathway after transtympanic injection, J. Nanobiotechnology. **13** (2015) 1. https://doi.org/10.1186/s12951-015-0065-9.
23. Lee, E. M., Lee J.,Kim Y.,Yi K. S.,Cho J., Kim J., An J. M., Lee D., Kim S. J., An E., Hong Y. J., Jo H., Lee S. H., Jung Y., Choi C.H.,Kang J. S.,Hur J.,and Kim D. - Hybrid Composite of Silver Nanoparticle-PorousSilicon Microparticles as an Image-Guided

Localization Agent for Computed Tomography Scan of the Lungs, ACS Biomater. Sci. Eng. **6** (2020) 4390. https://doi.org/10.1021/acsbiomaterials.0c00611.

24. Li, Z., Tian L., Liu J., Qi W., Wu Q., Wang H., Ali M. C., Wu W., and Qiu H. Graphene Oxide/Ag Nanoparticles Cooperated with Simvastatin as a High Sensitive X-Ray Computed Tomography Imaging Agent for Diagnosis of Renal Dysfunctions, Adv. Healthc. Mater. **6** (2017) 1700413. https://doi.org/10.1002/adhm.201700413.
25. S. Peng., Y. Lee., C. Wang., H. Yin., S. Dai., and S. Sun. -A facile synthesis of monodisperse Au nanoparticles and their catalysis of CO oxidation, Nano Res. **1** (2008) 229. https://doi.org/10.1007/s12274-008-8026-3.
26. L.T. Tam., N. H. Du., N. T. N. Linh., P. T. H. Tuyet., H. D. Quang., N. T. Vuong., L.T. t. Hiep., V. T. K. Oanh., L. D. Duong., L. T. Lu., T. D. Lam. - Facile Fabrication of Fe_3O_4@poly(acrylic) Acid Based Ferrofluid with Magnetic Resonance Imaging Contrast Effect, ChemistrySelect. **5** (2020) 12915. https://doi.org/10.1002/slct.202003015.
27. Hoa D. N., Tam T. L., Linh T. N. N., Tuyet T. H. P., Quang D. H., Nam H. P., Vuong T. N., Lu T. L., Lam D. T. Molecular Imaging Contrast Properties of Fe3O4-Au Hybrid Nanoparticles for Dual-Mode MR/CT Imaging Applications, ChemistrySelect. **6** (2021) 9389. https://doi.org/10.1002/slct.202102791.
28. Thanh N. T. K., Maclean N. A., Mahiddine S. - Mechanisms of nucleation and growth of nanoparticles in solution, Chem. Rev. **114** (2014) 7610. https://doi.org/10.1021/cr400544s.
29. Lu, L. T., Dung N. T., Tung L. D., Thanh C. T., Quy O.K., Chuc N.V., Maenosono S., and Thanh N. T. K.- Synthesis of magnetic cobalt ferrite nanoparticles with controlled morphology, monodispersity and composition: The influence of solvent, surfactant, reductant and synthetic conditions, Nanoscale. **7** (2015) 19596-19610. https://doi.org/10.1039/C5NR04266F.
30. Kathryn. M. M., and Jason H. H. - Localized surface plasmon resonance Sensors, Chem. Rev. **111** (2011) 3828. https://doi.org/10.1021/cr100313v.